Time-Dependent Capture Numbers with Repulsive Pair Interactions: Cu/Cu(111) and Ge/Si(001)

J. A. Venables[1,3], H. Brune[2] and J. Drucker[1]

[1]Department of Physics & Astronomy, Arizona State University, Tempe AZ 85287-1504, U.S.A.
[2]Institut de Physique des Nanostructures, EPFL, CH 1015 Lausanne, Switzerland.
[3]School of Chemistry, Physics & Environmental Science, University of Sussex, Brighton, U.K.

ABSTRACT

Recent experiments and calculations have shown that weak repulsive interactions between adsorbate atoms may shift nucleation kinetics from the well-known diffusion limit towards the attachment-limited case. The distinctions between diffusion- and attachment-limited kinetics are clarified, and the increased importance of the transient nucleation regime in the latter case is shown to be due to a combination of delayed nucleation and reduced capture. A time-dependent interpolation scheme between attachment- and diffusion-limited capture numbers is proposed, and tested against KMC simulations. Using this scheme to interpret recent STM results on Cu/Cu(111), bounds on the maximum adatom-adatom potential repulsive energy of 12±2 meV are deduced. Time-dependent effects also occur in the growth and ripening of strained Ge islands on Si(001), and the similarities and differences between these two systems are discussed.

RATE EQUATIONS CONTAINING SELF-CONSISTENT CAPTURE NUMBERS

Rate equations have been used successfully to analyze data, notably of the nucleation density n_x, as a function of experimental variables, usually the flux F (or equivalently deposition rate R) and the substrate temperature T [1-3]. The reaction rates in each equation, e.g. for the single adatom density n_1, are of the form $2\sigma_1 D_1 n_1^2$ (for the rate of adatoms forming pairs) or $\sigma_x D_1 n_1 n_x$ (for the rate of adatoms joining stable clusters). In these terms σ_1 and σ_x are *capture numbers*, and D_1 is the single-adatom diffusion coefficient. This paper discusses the determination of capture numbers, when there may be barriers for attachment of adatoms to other adatoms and to clusters. The full mathematical and computational details are given in a companion paper [4].

Although the distinction between *diffusion-limited* and *attachment-limited* kinetics is generally well known, there have not been many explorations of such issues in connection with epitaxial crystal growth. But several recent Scanning Tunneling Microscopy (STM) experiments at low temperatures on smooth metal surfaces [5,6] and associated *ab-initio* calculations [7,8] have highlighted attachment-limited behavior, due to the presence of repulsive barriers between adatoms. In particular, we show that capture numbers exhibit these two limits, and indicate how the two limits can be combined to give generally applicable, including time-dependent, forms.

Repulsive barriers modify the results of conventional (sometimes called classical) nucleation theory (CNT), by extending the transient nucleation regime to higher dose. New formulae are given for the capture numbers on the assumption of radial symmetry, and the expressions are tested against kinetic Monte Carlo (KMC) simulations. As a result, the maximum repulsive interaction energies can be reliably extracted from recent experiments on close-packed metal surfaces; here we concentrate on Cu/Cu(111). The methods may also be applied to other systems in future, and we compare our results qualitatively with Ge/Si(001).

DIFFUSION- VERSUS ATTACHMENT-LIMITED KINETICS

The Bessel function form of the capture numbers for the diffusion-limited case have been well known since the 1970's [9], but have not been uniformly applied in subsequent papers. This topic has been carefully evaluated in refs. [2] in the light of recent STM experiments and KMC simulations, especially for cluster size distributions $n_s(s)$ and spatial distributions. Attachment-limited kinetics has only been explored with rate equations to the authors' knowledge in one paper [10], and the formulation and conclusions are re-examined in [4]. In particular, we found that the problem can be formulated more generally, and that there are two sub-cases leading to rather similar results, shown in figure 1. Attachment-limited kinetics has been addressed recently via KMC simulations [8]. Some of their conclusions parallel ours from a different starting point.

In the first case shown in figure 1(a), there is an additional attachment barrier, of height E_B, at the interface of the growing island. This modifies σ_k (i.e. k =1, i, s or x, leading to σ_x for the average-sized cluster) by an attachment-barrier capture number σ_B, which add inversely as

$$\sigma_k^{-1} = \sigma_D^{-1} + \sigma_B^{-1}, \qquad (1)$$

where σ_D is the diffusion-limited capture number. The capture number σ_D is just the σ_k given by the normal diffusion solution, or uniform depletion approximation, but evaluated at $r = r_k+1$,

$$\sigma_D = (2\pi X_{k1}).K_1(X_{k1})/K_0(X_{k1}). \qquad (2)$$

The argument $X_{k1} = (r_k+1)/(D_1\tau)^{1/2}$ of the Bessel functions K_0 and K_1 sets the length scale where the adatom density is depleted in the vicinity of a k-cluster, which has radius r_k, in ML units of the jump distance. The barrier capture number σ_B is given simply by the single jump formula

$$\sigma_B = 2\pi(r_k+1)\exp(-\beta E_B) = (r_k+1)B, \qquad (3)$$

where the barrier parameter B is defined by the second equality in equation (3). The diffusion and barrier capture numbers add inversely as the diffusion flux across the barrier is conserved.

The specific case of complete condensation with i = 1 and 2D islands is illustrated in figure 2 (a) for one specific (D_1/F) value. The plot shows the capture numbers σ_x and σ_i, as a function of dose, for both the diffusion limited case (no barrier) and for three values of the barrier parameter $B = 2\pi\exp(-\beta E_B)$. Note that as the value of B is reduced, the capture numbers are reduced and become less dependent on dose, becoming dominated by the barrier capture number σ_B.

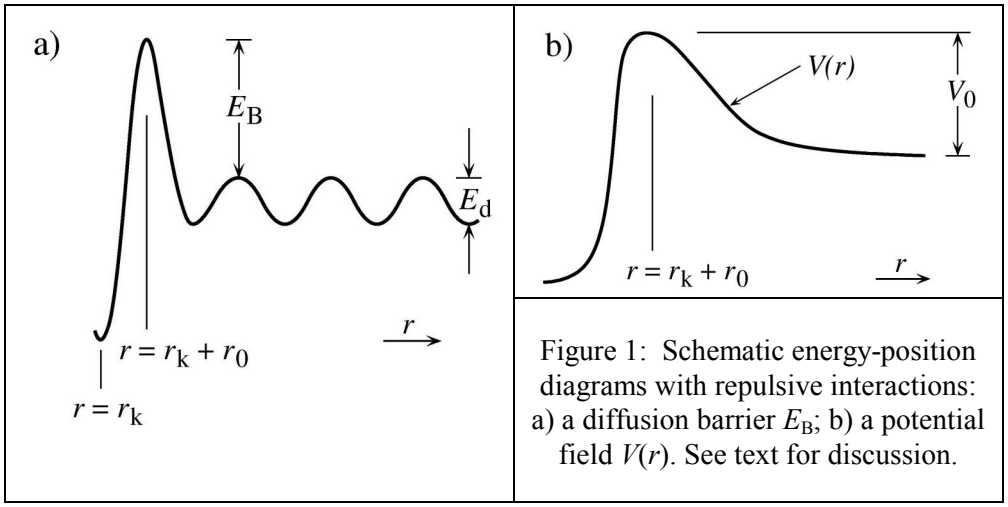

Figure 1: Schematic energy-position diagrams with repulsive interactions: a) a diffusion barrier E_B; b) a potential field $V(r)$. See text for discussion.

However, an additional important point is that steady state nucleation can be considerably delayed. This occurs because, with any or all of the capture numbers *reduced* by factors such as $\exp(-\beta E_B)$, the capture and/or nucleation times are *increased* by $\exp(+\beta E_B)$ to some power. Thus if the capture numbers (σ_1 *and* σ_x in the $i = 1$ case) are exponentially small, the transient regime can approach or even exceed 1 ML. Similarly, for larger critical sizes ($i > 1$), if the nucleation rate becomes exponentially small via a reduction in σ_i, this regime, where all the deposit is in the form of monomers and subcritical clusters, becomes greatly lengthened.

The longer transient regime is illustrated directly in the plots of n_1 and n_x as a function of dose θ in figure 2(b), for the same value of (D_1/F), and a wider range of $B = 2\pi\exp(-\beta E_B)$ values. It is seen that the transient regime (i.e. before the n_1 maximum, where $dn_1/d\theta = 0$) can be dominant for quite modest values of B; this is especially so at lower values of (D_1/F). In figure 2(b) for $(D_1/F) = 10^5$, the transient regime extends up to $\theta = 0.01$ ML for $B < 0.1$. This trend has been followed [4] both to higher ($D_1/F = 10^7$) and particularly to lower ($D_1/F = 10^3$ and 10) values, where it is well known that the transient regime is extensive even without barriers.

CAPTURE NUMBERS WITH LONG-RANGE REPULSIVE INTERACTIONS

The second case, illustrated schematically in figure 1(b), arises when the individual adatoms and/or clusters have repulsive potential energy fields $V(r)$ around them, with a range exceeding one lattice distance; the diffusion barriers are not shown in the figure. Here it is primarily the change in energy landscape that is crucial in reducing $n_1(r)$ in the neighborhood of other adatoms and clusters, though this could also influence the adatom diffusion constant D_1, which can then depend on r. For this case, a different starting point is needed [4]. As outlined below, the quantity $V_0 = V(r_k+r_0)-V$, where the maximum is at $r = r_k+ r_0$ and V is the value at large r, plays a role similar to E_B in the first case, if for different (thermodynamic not kinetic) reasons.

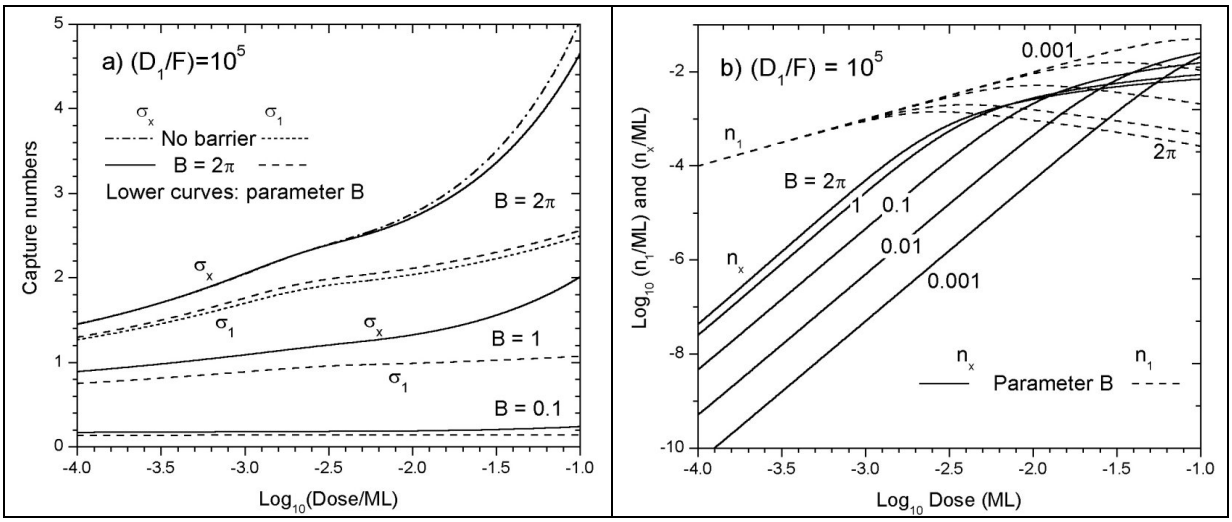

Figure 2: a) Capture numbers σ_x (full lines) and σ_i (dashed lines, for $i = 1$) as a function of dose, for three values of the barrier parameter $B = 2\pi\exp(-\beta E_B) = 2\pi$, 1 and 0.1, for $(D_1/F) = 10^5$;
b) Log-log plots of n_1 and n_x as a function of dose, θ, with a wider range of B values as indicated. Note the increased importance of the transient regime for lower values of B, where $n_1 = \theta$, and n_x is roughly proportional to θ^3 for $i = 1$. See text for discussion and ref [4] for detailed conditions.

With a repulsive potential $V(r)$, we need to evaluate the response to concentration ($\nabla n_1(r)$) and potential ($\nabla V(r)$) gradients, via consideration of phenomenological transport coefficients, which leads to a more general definition of the particle flux $\boldsymbol{j}(\mathbf{r})$ in terms of chemical potential gradient $\nabla\mu(\boldsymbol{r})$. We can formulate this problem in terms of the chemical diffusion coefficient D and the tracer diffusion coefficient D^*, to produce a general expression [4] for $\boldsymbol{j}(\mathbf{r})$ as

$$\boldsymbol{j}(r) = -D\nabla n_1(r) - (n_1(r)D^*)\beta\nabla V(r). \qquad (4)$$

This expression is true in general, but it cannot be solved without further approximation. At low concentrations, we can deduce the corresponding capture number, since $D = D^* = D_1$, to obtain

$$\sigma_k = [2\pi(r_k+r_0)(-\beta\nabla V(r_k+r_0)) + 2\pi X_{k0}.(K_1(X_{k0})/ K_0(X_{k0}))].\exp(-\beta(V(r_k+r_0)-V)). \qquad (5)$$

Here the argument $X_{k0} = (r_k+r_0)/(D_1\tau)^{1/2}$ is evaluated at the maximum of the potential shown in figure 1(b), which occurs at a distance r_0 from the cluster edge. Note that the diffusion-limited capture number (the second term in 5) is reduced relative to expression (2) by the Boltzmann factor $\exp(-\beta V_0)$, where $V_0 = V(r_k+r_0)-V$; this reduction is substantial for high values of βV_0.

The first term of equation (5) is an attachment limited term, $\sigma_B = 2\pi(r_k+r_0)C\exp(-\beta V_0)$, where C is a constant, although, if $V(r)$ has zero gradient at the maximum where $r = r_k+r_0$, then $C = 0$. However, during the transient stage, before any spatial correlations have developed, this form of the capture numbers is dominant, with $C = 1$, or written in the same form as equation (3)

$$\sigma_B = 2\pi(r_k+r_0)\exp(-\beta V_0) = (r_k+r_0)B_V, \qquad (6)$$

where B_V is the 'barrier' parameter due to the potential field. Thus, in both cases illustrated in figure 1, and depending on the initial conditions, there may be an explicit time-dependence to the capture numbers. Over time, spatial correlations develop; thus the full expression requires an interpolation formula to chart the reduction in the barrier-like contribution, and its replacement by the diffusion solution, the second term of equation (5).

TIME-DEPENDENT CAPTURE NUMBERS FOR Cu/Cu(111)

We illustrate these points with a single example, Cu/Cu(111), for which it is known we are dealing with complete condensation, $i = 1$, and small 2D islands [5,6]. Here we concentrate on an interpolation scheme to model the capture numbers in the transient regime. The details of the *in-situ* low temperature STM experiments, at $T = 16.5$ K at a flux $F = 5.10^{-3}$ ML/s, are given in [6]. From previous work we know that the diffusion energy E_d of Cu adatoms = 40 ±1 meV, with a pre-exponential frequency factor $\nu = 10^{12\pm0.5}$ s^{-1}, yielding $D_1 = 0.156$ ML/s. These values give (D_1/F) approximately equal to 30 during deposition, and a final dose $\theta = 0.0014$ ML.

At such a low dose and value of (D_1/F), almost all of the deposited material is in the form of monomers, and the few existing clusters are in the form of dimers. Using computed values at the end of deposition, progress of n_1, n_x was followed during annealing, for $r_0 = 1.25$, chosen to agree with the initial values in the KMC data. Cluster formation can be seen by the rise in n_x which accompanies the fall in n_1 as a function of $(D_1t)^{0.5}$, with parameter B_V. The absolute values of n_1 and n_x, and especially the ratio (n_x/n_1), are sensitive tests of model parameters.

The steady state mean field capture numbers were initially used with this range of B_V values, corresponding to $0 < V_0 = E_B < 10$ meV. As seen in figure 3(a), dashed curves, this leads us to underestimate the amount of annealing. Initially the capture number is the given by the pure attachment limit, equations (3) or (6). The curves for 5 and 10 meV are in essential agreement

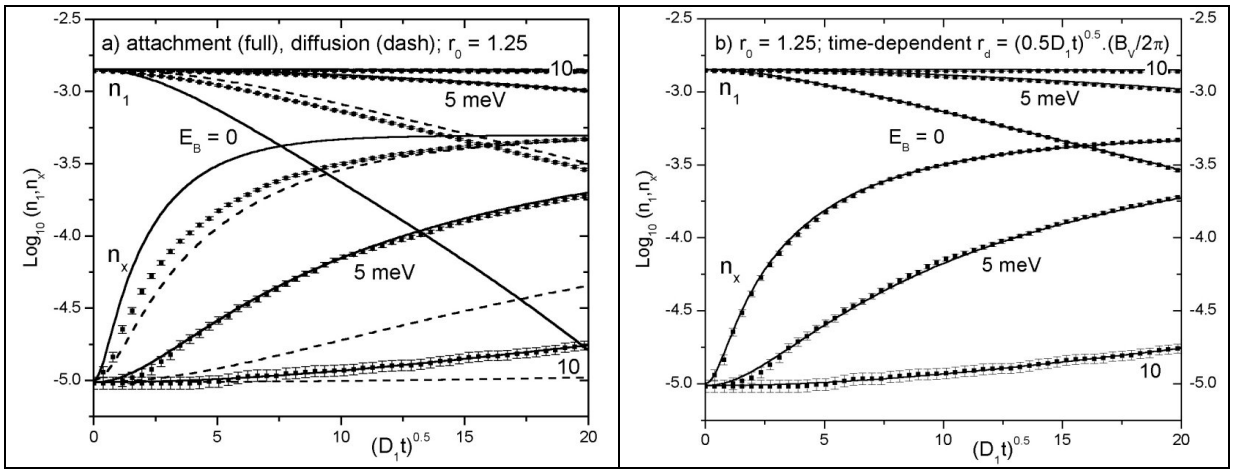

Figure 3: Predicted n_1 and n_x annealing curves for Cu/Cu(111) as a function of $(D_1t)^{0.5}$, with attachment barriers $V_0 = E_B = 0$, 5 and 10meV, compared to KMC (squares with error bars): a) attachment-limited (full lines) and diffusion limits (dashed lines); b) time-dependent interpolation scheme between attachment and diffusion solutions. See text for discussion.

with this simple formula over the whole range of annealing conditions shown in figure 3(a); they would also be in perfect agreement for all larger values of V_0 or E_B; but for larger energies there is almost no annealing over the range of (D_1t) shown. On the other hand, equation (3) or (6) gives far too much annealing when $V_0 = E_B = 0$, most clearly seen in figure 3(a) by the gross discrepancy in the prediction of n_1. Thus for the lower values of V_0 or E_B, or for longer annealing times, an interpolation scheme is needed, which takes the capture number from the uncorrelated value to a diffusive value over the correct range of (D_1t) and the other parameter, B or B_V.

A particular set of the interpolated curves is shown in figure 3(b), based on the formula

$$\sigma_k = (\sigma_B f_t) f_t + \sigma_{kd}(1-f_t), \qquad (7)$$

where σ_{kd} is the diffusive contribution given by the second term of equation (5), and f_t is a transient factor, such that at $(D_1t) = 0$, $f_t = 1$, and as $(D_1t) \rightarrow \infty$, $f_t \rightarrow 0$. The physical argument used is that the transient is due to capture from a diffusion zone around the adatom or cluster considered, whose radius r_d increases with time as a linear function of $(D_1t)^{0.5}$ and B_V. The details are given in [4], where it is also shown that we can use equation (7) to extrapolate to higher temperature annealing, and by comparison with experiment, determine V_0 as 12±2 meV.

COMPARISON OF Ge/Si(001) WITH Cu/Cu(111)

It is instructive to consider the relationship between the relatively simple sub-ML Cu/Cu(111) system, and the much more complex Ge/Si(001) system at multi-layer coverage. The (2x1) and related superstructures on Si and Ge(001) arise from the strong dimer bonds which reduce the number of dangling bonds. Most of the sublimation energy, L = 4.63±0.04 eV/atom, is gained by formation of surface dimers, and very little extra energy remains to be gained when these dimers are incorporated into the growing crystal. These ad-dimers have low formation energy, E_{f2}, measured for Si/Si (001) as 0.35±0.05 eV [3,11]. These energies show that, although the Si and Ge(001) growth systems may be close to 2D equilibrium, they are very far from equilibrium with their (3D) vapor at normal growth temperatures, 450-650 ^{0}C. This has encouraged a ‘classical’

treatment of nucleation and growth in terms of edge energies for 2D nuclei; critical nucleus sizes up to $i = 650$ have been deduced in some cases; this approach has been reviewed recently [12].

Most interest has focused on the growth of clusters above a wetting layer, which is 3ML thick for pure Ge grown on Si(001) [3,13]. There are many other relevant details, especially the role of strain energy, which increases with island size until coherence is lost by introducing misfit dislocations, and various types of islands, surrounded by trenches for strain relief at higher temperatures [14]. At lower temperature, the wetting layer thickness can be > 3 ML, but extra layers are metastable, and disappear on annealing, especially rapidly once dislocated islands have formed, due to dimer diffusion energies of ~ 1 eV. In the present context, it seems worthwhile to explore the idea that capture numbers are reduced for strained islands, and that the transient regime might extend to a coverage > 1ML for realistic parameters, which give large *i*-values. This is work in progress; a brief survey in the context of quantum dots is given in [15].

To summarize this comparison of Ge/Si(001) and Cu/Cu(111): we have found the transient regime can be substantially lengthened when there are repulsive interactions between adatoms, and requires time-dependent capture numbers. This regime contains a finite number of adatoms, and so is important for the early stages of sub-ML growth as in Cu/Cu(111), or when large critical nucleus sizes delay nucleation substantially, as expected for Ge/Si(001). Annealing is shown to be especially sensitive to low capture numbers, which delay coarsening substantially.

REFERENCES

1. J.A. Venables, *Surface Sci.* **299/300**, 798 (1994).
2. H. Brune, *Surface Sci. Rep.* **31**, 121 (1998); H. Brune, G.S. Bales, J. Jacobsen, C. Boragno and K. Kern, *Phys. Rev. B* **60**, 5991 (1999).
3. J.A. Venables, *Introduction to Surface and Thin Film Processes* (CUP, 2000), chaps 4, 5 & 7.
4. J.A. Venables and H. Brune, *Phys. Rev. B* **66**, 195404 (2002).
5. J. Repp, F. Moresco, G. Meyer, K-H. Rieder, P. Hyldgaard and M. Persson, *Phys. Rev. Lett.* **85**, 2981 (2000).
6. N. Knorr, H. Brune, M. Epple, A. Hirstein, M.A. Schnieder and K. Kern, *Phys. Rev. B* **65**, 115420 (2002).
7. A. Bogicevic, S. Ovesson, P. Hyldgaard, B.I. Lundqvist, H. Brune and D.R. Jennison, *Phys. Rev. Lett.* **85**, 1910 (2000); S. Ovesson, A. Bogicevic, G. Wahnström & B.I. Lundqvist, *Phys. Rev. B* **64**, 125423 (2001); S. Ovesson, *Phys. Rev. Lett.* **88**, 116102 (2002).
8. K.A. Fichthorn and M. Scheffler, *Phys. Rev. Lett.* **84**, 5371 (2000); K.A. Fichthorn, M.L. Merrick and M. Scheffler, *Appl. Phys. A* **75**, 17 (2002).
9. J.A. Venables, *Phil. Mag.* **27**, 697 (1973) and references quoted.
10. D. Kandel, *Phys. Rev. Lett.* **78**, 499 (1997).
11. R.M. Tromp and M. Mankos, *Phys. Rev. Lett.* **81**, 1050 (1998).
12. W. Thies and R.M. Tromp, *Phys. Rev. Lett.* **76**, 2770 (1996); R.M. Tromp and J.B. Hannon, *Surface Rev. Lett.* **9**, 1565 (2002).
13. M. Krishnamurthy, J.S. Drucker and J.A Venables, *J. Appl. Phys.* **69**, 6461 (1991); J. Drucker, *Phys. Rev. B* **48**, 18203 (1993).
14. S.A. Chaparro, Y. Zhang, J. Drucker, D. Chandrasekhar and D.J. Smith, *J. Appl. Phys.* **87**, 2245 (2000); S.A. Chaparro, Y. Zhang and J. Drucker *Appl. Phys. Lett.* **76**, 3534 (2000).
15. J.A. Venables, P.A. Bennett, H. Brune, J. Drucker and J.H. Harding, *Phil. Trans. R. Soc. Lond.* A **361**, in press (2003), and work in progress.